

Binding of Alkaline Earth Halide Ions MX^+ to Benzene and Mesitylene

Alexei Gapeev and Robert C. Dunbar*

Chemistry Department, Case Western Reserve University, Cleveland, Ohio 44106

Received: December 13, 1999; In Final Form: February 15, 2000

The binding energies of M^+ and MX^+ ions to benzene and mesitylene were measured by the radiative association kinetics approach in the Fourier transform ion cyclotron resonance (FT-ICR) spectrometer, where M was Mg, Ca, or Sr and X was Cl or Br. MCl^+ binds to the aromatic face roughly half again as strongly as the corresponding M^+ ion. (For instance, 2.6 eV vs 1.6 eV for $\text{MgCl}(\text{benzene})^+$ vs $\text{Mg}(\text{benzene})^+$.) This is true for all three metals, although the absolute magnitude of the binding energy decreases sharply in going from Mg to Ca to Sr as a consequence of decreasing electrostatic interaction. Bromide has a smaller effect on the binding ability of the metal center than chloride, in keeping with its lower electron-withdrawing ability. Quantum chemical calculations for MgCl^+ are in accord with the measured binding energy and also show the expected decrease of the metal–ring bond distance in going from Mg^+ to MgCl^+ . The qualitative picture is presented that MX^+ behaves as a metal ion center with the charge of a monovalent ion but the electronic character of a divalent alkaline earth cation. The calculations indicate that the gas-phase binding of MX^+ ions to the aromatic face is intermediate between the binding abilities of M^+ and M^{2+} . In the particular case of MgCl^+ , quantitative analysis via quantum chemical calculations indicates that this ion binds in a manner equivalent to a hypothetical magnesium center with fractional charge of +1.3 to +1.4. A second aromatic ligand normally adds to the monomer complex. Radiative association kinetics analysis indicates that the second ligand is bound with energy comparable to, or somewhat less than, the first ligand, and substantially less in the magnesium cases.

Introduction

There has been extensive consideration over the years of the effect on metal ion reactivity of adding electronegative atoms to the bare metal ion. For example, addition of oxygen,^{1–3} sulfur,⁴ or chloride⁵ to a metal center has been found to enhance the reactivity. Also interesting is work on CrF_n^+ , showing enhanced reactivity toward alkanes of the more highly fluorinated species.⁶ Considering the energetics of metal–ligand binding in cases where the bound complex does not undergo further reaction, most reports have addressed the effect of one weakly perturbing ligand on the binding of another ligand. A lot of work has been done on this question with σ - and π -donor ligands such as CO, H_2O , alkenes, benzene, cyclopentadienyl, etc.^{7–9} On the other hand, there has not been much consideration of how a highly electronegative atomic substituent like halogen affects the binding ability of the metal center toward σ - or π -donor ligands. One recent example, involving chalcogenide atom substituents, showed that attachment of O or S to Mo^+ increased the binding energy to a chalcogenide ligand by $\sim 10\%$.³ The present work examines the effect of halide ion substitution on metal ion binding to a π ligand. It offers a novel perspective of how the MX^+ ion (M = metal, X = halogen) compares with M^+ in its binding behavior toward the prototypical π ligand benzene.

In solution, the doubly charged alkaline earth ions bind to basic sites in a variety of contexts. Drawing gas-phase analogies and models for this binding is not directly possible, because in the gas phase the absence of the leveling effect of water leads to strong electrostatic attractions between M^{2+} and neutral ligands that have no counterpart in aqueous solution. An added

problem beyond this fundamental difference between aqueous solution and gas phase is that charge transfer to form ($\text{M}^+ + \text{L}^+$) is normally an exothermic reaction. Thus, gas-phase M^{2+} –L complexes are normally not thermodynamically stable and are problematic as subjects for gas-phase experimental study. In making parallels between binding in a vacuum and aqueous environments, it is more attractive to look to the gas-phase complexes of M^+ , rather than those of M^{2+} . However, the alkaline earth M^+ ions are poorly analogous to solution M^{2+} ions, since the unpaired electron in the outer s shell of M^+ is likely to dominate the ion–ligand interaction in ways unrelated to the interactions relevant to solution binding. Following the theme of gas-phase ion–neutral complexation chemistry with more useful connections to aqueous M^{2+} chemistry, it is interesting to explore the behavior of the MX^+ ions, where M is an alkaline earth (Mg, Ca, or Sr) and X is a halogen (Cl or Br). The MX^+ ion has a formal oxidation state of +2 for the metal center and might be expected to be analogous to M^{2+} in terms of its electronic character. In simplistic terms, we want to take the point of view that MX^+ represents a gas-phase reagent ion with the electronic character of an M^{2+} ion, but with electrostatic characteristics closer to a singly charged ion.

Considering the question of MX^+ binding to benzene from the point of view purely of its gas-phase complexation behavior, we can put this work in another context: The binding of M^+ to benzene represents one extreme (weak binding) of a continuum of binding effects, along which the binding of M^{2+} represents the other (strong-binding) extreme. Along this continuum of behavior, MX^+ represents an intermediate situation. We can develop this idea by considering the MX^+ ion as a metal-like ligand whose effective charge is intermediate between singly

* To whom correspondence should be addressed.

and doubly charged and whose binding energy is expected to be correspondingly intermediate between Mg⁺ and Mg²⁺.

There are a wide variety of methods for experimental determination of metal–ligand binding energies. Among those in frequent use we may note (1) methods based on dissociation energetics, using threshold collision-induced dissociation,⁷ competitive collision-induced dissociation (kinetic method),^{10,11} threshold photodissociation,^{12–14} photodissociation kinetics,^{15–17} blackbody IR dissociation,^{18–22} and IR multiphoton dissociation;^{17,23,24} (2) methods based on ligand exchange, either involving true equilibrium,²⁵ or thermochemical bracketing by exothermic reactions; and (3) methods based on association, using radiative association^{17,26} or associative equilibrium.²⁷ The approach currently used in our laboratory, which is convenient for the present systems, is based on the third of these strategies and involves the kinetic analysis of radiative association at very low pressure. When the pressure is low enough so that collision-stabilized association is negligible, an ion–neutral complex may be formed by the radiative process



where AM^{+*} is a metastable ion that can redissociate to reactants or form a stable complex with emission of a photon (usually in the IR spectral region). The kinetics of complex formation depend strongly, in a well understood way, on the binding energy, and kinetic analysis provides a practical and fairly precise way to obtain both relative and absolute ion–neutral binding energies. Among recent studies exploiting this approach, a number have addressed complexes with metal ions.^{28–33}

Experimental Section

The measurement of the radiative association rate constants was similar to other recent work in our laboratory. The instrument was a modified Nicolet Fourier transform ion cyclotron resonance instrument having a 3 T magnet. A single-region 5 cm cubic cell was used. Data handling was done by an IonSpec Omega data system. The vacuum system was pumped to a base pressure below 10^{−9} Torr (as indicated by the ionization gauge) by a cryopump. The benzene or mesitylene reactant was introduced through a leak valve, and pressures were measured by an ionization gauge. The benzene pressure was referred to a calibration established for this instrument based on known ion–neutral reaction rate constants. Neutral reactant pressure was typically in the range (3–7) × 10^{−8} Torr.

With mesitylene, the cell pressure was not tracked in a stable and reproducible way by the ionization gauge, and satisfactory kinetic results could not be obtained using this pressure measurement approach. To overcome this problem, we used an “internal pressure calibration” approach employing Ni⁺ as an internal standard: we assumed that bare Ni⁺ cations and mesitylene react with a rate approaching the Langevin orbiting rate. Accordingly, nickel cations were produced simultaneously with alkaline metal halogenide ions and their reaction rate with mesitylene was monitored in each run.

The preparation of gas-phase MX⁺ ions in the FT-ICR ion trap presents a challenge. The scope of the present work was somewhat constrained by the limited set of reagent ions we were able to synthesize while maintaining satisfactory conditions in the cell. The MX⁺ species were prepared via ion–molecule reaction between singly charged bare metal cations and a halogen source. Iodine monochloride (ICl) and chloroform were equally effective for forming the chlorides, and bromoform was

used to form the bromides. The neutral reagent, whether ICl, chloroform, or bromoform, was introduced through a pulsed valve in a short pulse immediately following the laser shot, and a substantial fraction of the initial metal ions were converted to the halide. After the pulse of reagent gas died away, an ejection sequence was used to remove residual metal ions and other unwanted ions before the beginning of the kinetics determination. A second or two after the laser pulse the reagent neutral pressure had fallen to negligible levels, and further reactions of the reagent compound were not observed. The one exception to this was MgBr⁺, which reacted with another CHBr₃ molecule forming CBr₄⁺ with such high efficiency that the interference of this process could not be overcome. For this reason kinetic results for MgBr⁺ were not obtained.

For some of this work, bare singly charged alkaline-earth metal ions were generated by laser desorption–ionization from a metal target. An alternative method was to use a pressed mixture of metal salts (carbonates or chlorides) as a target, from which the laser shot typically produced abundant metal ions (but, unfortunately, no metal–salt ions). In experiments using this latter approach, as many as three different metal cations were simultaneously present in the cell, permitting direct competitive comparisons between different metals. In particular, this approach was always used in the mesitylene experiments so that Ni⁺ could be maintained as an internal standard in all these experiments. Various comparisons of pairs of reactions with benzene by direct competition and by separate measurements gave relative rate constants among different ionic reactants that were stable, consistent and reproducible. Following the standard methodology for kinetic studies in the FT-ICR ion trap, the intensities of metal halogenide ions and the intensities of product ions were monitored as a function of reaction time in order to derive the association rate constants. The successive additions of the first and second ligands to the MX⁺ ion were fitted to a sequential kinetic scheme, and the rate constants of the two processes were obtained from the fit.

Kinetic Analysis

The treatment of radiative association rate constants to obtain the corresponding binding energies has been described several times in detail.^{17,26,30,34} We have commonly used two approaches: one, an estimation scheme referred to as the standard hydrocarbon model (SHM)^{35–37} assigns generic properties to the complex, allowing useful though approximate estimates of binding energy based on the temperature, the size of the complex (number of degrees of freedom), and the observed association efficiency.

More accurate, when it can be carried out, is the analysis of the kinetics by variational transition state theory (VTST), using vibrational frequencies and infrared emission intensities that are calculated *ab initio*, obtained from experiment, or otherwise estimated.^{34,38} The VTST approach, implemented using the VariFlex kinetics package,³⁹ was used for the monomer complexes of benzene. For the dimer complexes, and for all the mesitylene complexes, the SHM estimation method was used.

In the paper describing the most recent SHM parametrization,³⁵ it was noted that a correction factor might be appropriate when one of the reactants is a diatomic, analogous to the established correction for an atomic reactant. However, there was insufficient evidence at that time to justify establishment of such a correction. In the course of the present work, several cases involving the diatomic MX⁺ reactant ion were calculated using both *ab initio*/VTST analysis and also SHM analysis, and

TABLE 1: Kinetics Results and Corresponding Derived Binding Energies for the Complexes

ion	neutral	<i>T</i> (°C)	<i>k</i> (monomer) ^a	<i>k</i> (dimer) ^a	BE _{mono} (eV) ^b	BE _{dimer} (eV) ^b
Mg ⁺	benzene	25	4.2 × 10 ⁻¹²	none	1.61 , 1.5	<1.4
MgCl ⁺	benzene	25	1.1 × 10 ⁻⁹	none	>2.5 ^c	<1.4
		45	5.5 × 10 ⁻¹⁰		2.70	
		83	5.3 × 10 ⁻¹⁰		2.79	
		110	1.8 × 10 ⁻¹⁰		2.56	
		143	1.6 × 10 ⁻¹⁰		2.63	
MgCl ⁺	mesitylene	25	fast	3.0 × 10 ⁻¹¹	>2 ^c	1.5
Ca ⁺	mesitylene	25	2.0 × 10 ⁻¹⁰	2.4 × 10 ⁻¹¹	1.4	1.3
CaCl ⁺	benzene	25	2.5 × 10 ⁻¹¹	8.3 × 10 ⁻¹²	1.86 , 2.0	1.5
CaCl ⁺	mesitylene	25	9.5 × 10 ⁻¹⁰	1.9 × 10 ⁻¹⁰	~2 ^c	1.6
CaBr ⁺	mesitylene	25	1.9 × 10 ⁻¹⁰	2.5 × 10 ⁻¹¹	1.7	1.4
Sr ⁺	mesitylene	25	1.4 × 10 ⁻¹¹	6.5 × 10 ⁻¹²	1.2	1.2
SrCl ⁺	benzene	27	3.2 × 10 ⁻¹²	1.9 × 10 ⁻¹¹	1.57 , 1.8	1.6
SrCl ⁺	mesitylene	25	2.3 × 10 ⁻¹⁰	1.8 × 10 ⁻¹⁰	1.7	1.5
SrBr ⁺	mesitylene	25	1.1 × 10 ⁻¹⁰	2.0 × 10 ⁻¹¹	1.6	1.3

^a cm³ molecule⁻¹ s⁻¹. ^b Boldface values derived by full VTST calculation. Italicized values from SHM (ref 35), modified as discussed in the text. The VTST-derived binding energies are probably uncertain in absolute value by ±15%, and the SHM-derived values are more uncertain. Comparisons between values in the table should have smaller uncertainty, so that a difference of even 0.1 eV between two values may be slightly significant. ^c These rates are so close to the collision limit that any estimate or lower limit is at best highly approximate.

it was found that the SHM binding energies were consistently higher than the values derived by VTST. There seemed to be sufficient basis to justify a diatomic reactant correction, at least for the present systems. The correction used was to divide the SHM-derived binding energy by a factor of 1.2 when the reactant ion was diatomic. (This compares with the corresponding factor of 1.4 established for the atomic reactant correction.³⁵)

A feature of the association kinetics approach to determining binding energies is that if the association rate constant is close to the collision rate a saturation effect reduces the precision of the analysis. Thus, for instance, the association of MgCl⁺ with benzene at room temperature proceeds with nearly collisional efficiency, and provides only very rough binding energy information. However, this particular reaction was also studied at higher temperatures where the rate constant is lower, allowing the assignment of a more precise binding energy. The saturation problem limited our ability to assign precise binding energies in several cases, as noted below.

Results and Discussion

For all of the systems described here, association with the aromatic substrate was the only significant ion–neutral reaction observed for the metal-containing ion, so that determination of the association rate constants from the data was entirely straightforward. Table 1 shows the rate constants measured for radiative association of the metal ions and the metal halides with benzene and mesitylene, as well as the rate constants for addition of a second ligand to form the dimer complexes. Where possible, the kinetics were analyzed by the full VTST approach to give corresponding binding energies (boldface values). In the other systems, binding energies were estimated by the SHM scheme (italicized values).

The only case for which a reliable literature value of binding energy exists for comparison is Mg(benzene)⁺. Armentrout's group recently measured this binding energy by the threshold CID approach, which is considered reliable, obtaining a binding energy of 1.39 eV. This is lower than the present value of 1.61 eV, although the difference is not outside the realistic uncertainty of the measurements and analysis.

M⁺ vs MX⁺. The principal theme of this work is that MX⁺ binds to π systems much more strongly than M⁺, which is very evident from Table 1. For MgCl⁺, the difference is about 1.0 eV. For CaCl⁺ and SrCl⁺ the difference is less, of the order of 0.5 eV. For chlorides of all three metals, the binding energy increases by roughly half upon adding the chlorine. The chloride effect in the MgCl⁺ case is analyzed in more detail below.

Effect of Neutral Partner. It would be expected that binding energies would be similar for the same ionic species binding to benzene or to mesitylene, which provides the chance to assess the internal consistency of the radiative association kinetics analysis. Since the rate constants for corresponding benzene and mesitylene systems are very different (on account of the differing number of internal degrees of freedom), the extraction from them of similar binding energies is a significant check on the analysis. The data set offers a limited number of such comparisons. For the monomer complexes, SrCl⁺ is the only species with reasonably precise values for both neutrals, and it is seen that the binding energies are indeed the same within the precision of the analysis. For CaCl⁺ the values estimated for both neutrals are similar, but this has limited significance since the CaCl⁺/mesitylene value is highly approximate. For the dimer complexes, there is good agreement for both the CaCl⁺ and SrCl⁺ cases. For MgCl⁺, the failure to observe the dimer complex for benzene is consistent (within the uncertainty) with the binding energy estimate of 1.5 eV from mesitylene.

Effect of Metal Ion. Going down the period from Mg to Ca to Sr, the increasing size of the metal ion leads to a sharp drop-off in electrostatic binding energy contributions. This drop-off is very obvious in Table 1 when comparing the monomer binding of any given ionic species as a function of the metal. Ca-containing complexes are considerably weaker than corresponding Mg species, while Sr-containing complexes are significantly weaker than Ca species.

Interestingly, the dimers show less variation as a function of metal ion. We can speculate that the steric crowding around the ionic center decreases as we go to the larger metals, giving a decrease in steric repulsion that tends to compensate for the drop-off in electrostatic binding attraction.

Bromide vs Chloride. The data for both CaX⁺ and SrX⁺ suggest that replacing Cl with Br gives a small reduction in binding energy for monomers, although the MBr⁺ binding is still significantly stronger than for the bare metal M⁺. The smaller effect of Br compared with Cl is qualitatively as expected, reflecting the lower electronegativity of Br and the consequent lower effective charge on the metal center in the MBr⁺ ions relative to MCl⁺.

For the dimers, the RMBr⁺ ions appear to bind the second ligand slightly less strongly than the RMCl⁺ ions, and in fact, the R–MBr⁺ binding is not different from R–MR⁺ within the precision of our results. There is a serious likelihood of steric crowding and weakening of the binding for the R–MBr⁺ dimer complexes, where there are three bulky ligands around the metal center. Thus, it is hard to draw meaningful conclusions from the dimer comparisons among different MBr⁺ cases, or comparisons of bromide versus chloride dimer complexes.

Dimers vs Monomers. With the exception of Mg⁺ and MgCl⁺ with benzene, a second ligand adds with measurable rate to produce the dimer complex in all cases. Surveying Table 1, it is seen that the second-ligand binding energies for Ca and Sr systems are generally of the same order of magnitude as the monomer binding energies, while for the Mg systems second-ligand addition is much less favorable. The dimer binding energies appear to be systematically lower than the monomer

TABLE 2: Calculated Binding Properties of Mg Complexes^a

	Mg–ring distance (Å)	Mg–Cl distance (Å)	binding energy (eV)
Mg(benzene) ⁺	2.32		1.38
Mg(benzene) ⁺²	1.95		5.15
MgCl(benzene) ⁺	2.09	2.16	2.54
MgCl ⁺		2.13	

^a B3LYP-DFT, basis set 6-31+g(d) on heavy atoms, 6-31g(d) on H. Geometries fully optimized.

energies by small amounts, particularly for the mesitylene cases. It is easy to suppose that steric crowding around the metal could become important for MX(mesitylene)₂⁺ complexes and for complexes involving the small Mg center, and could lead to a decrease in binding energy of the second ligand. It is also true that the second ligand cannot approach the metal atom in the most favorable location opposite the halide atom, and it could be expected that it would bind much less strongly on this account. It is thus reasonable to attribute the observed effect to a combination of steric crowding and electronic effects. It is perhaps surprising that the second ligand binds as strongly as is observed in the Ca and Sr systems.

Nature of Binding in MgCl(benzene)⁺. The results discussed above show clearly that MX⁺ is much more strongly bound to benzene than M⁺, just as expected from the increase in formal oxidation state from +1 to +2. This does not, however, show us how closely the metal center approaches the binding behavior of an actual M²⁺ ion. Experimental information on M(benzene)⁺² complexes is not available, and it is not even certain that such complexes are observable, since they can exist only by virtue of a local potential minimum and can dissociate exothermically to (M⁺ + benzene⁺). Quantum calculations offer a useful way to get more insight into the nature of the binding in these complexes, and to address such questions. Following this idea, detailed calculations were carried out for Mg⁺, Mg²⁺, and MgCl⁺ with benzene, which are small enough systems so that all-electron density functional (DFT) calculations with an adequate basis set are not difficult and are expected to be sufficiently accurate and reliable for our purposes. The Mg²⁺ calculations showed no tendency to cross over to the exothermic (Mg⁺ + benzene⁺) exit channel, and there was no difficulty in converging to a stable Mg²⁺(benzene) species. The computed results for the equilibrium complexes are shown in Table 2. The calculations at other Mg–ring distances were carried out with similar methods, except that the geometry of the ligand was frozen at the equilibrium-complex geometry. The Gaussian 94 quantum chemistry program suite was used⁴⁰ to carry out B3LYP density functional calculations. It is encouraging that the calculated binding energy of MgCl⁺/benzene (Table 2) is in good accord with the measured value (Table 1).

It has been said⁴¹ that the binding of Mg⁺ to benzene is largely electrostatic (using the term “electrostatic” to include both the static charge–multipole interactions and also the charge–polarizability interactions between the ion and neutral). This is certainly an oversimplification, and there are undoubtedly binding contributions of covalent character, as well as stabilization by charge transfer electron delocalization, to the actual binding. However, the electrostatic picture gives a useful semiquantitative understanding of the binding, and the other contributions are apparently relatively small.

The calculations displayed in Figure 1 were undertaken as an indication of how well the pure electrostatic picture does actually account for the attractive interaction and the total binding energy in the Mg⁺ and Mg²⁺ cases. The points labeled “Potential” are the DFT results for the energy of the system

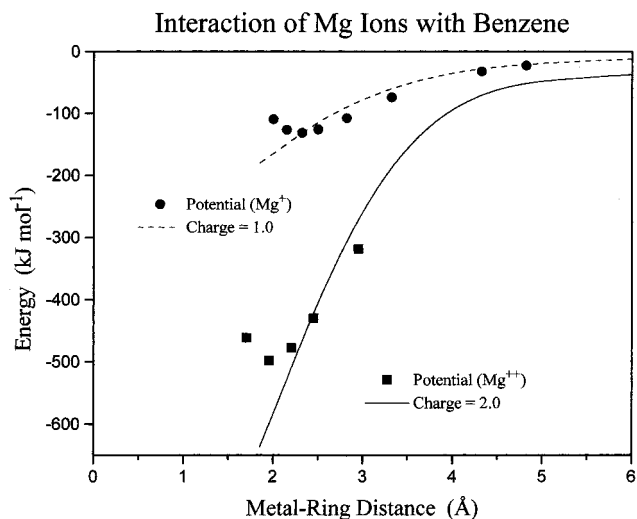


Figure 1. Computed (DFT) interaction energies of singly and doubly charged Mg ions with benzene. Data points are binding energies from full calculations of the actual complex, while the solid and dashed curves are model calculations in which the metal ion is replaced by a point charge.

(relative to separated partners) as a function of metal–ring distance. The lines show the calculated “pure electrostatic” interaction, calculated using DFT calculations for neutral benzene in the electric field of a point charge (either +1 or +2) placed at the same point that the metal ion would occupy. These latter values thus represent all of the electrostatic (charge–multipole plus polarization) interaction between an ideal point-charge metal ion and benzene.

It can be seen that for both charge states, the electrostatic contribution is a fair approximation to the actual potential curve as the ion moves toward the equilibrium binding position r_e . At distances larger than r_e , the electrostatic curve somewhat underestimates the binding energy, which is a reflection of the contributions of other effects such as charge transfer, electron delocalization and the non-point-charge nature of the ion. The curves suggest that these effects are modest compared with the basic electrostatic energy. As r_e is approached, the repulsive interactions (steric repulsions) between the electron clouds of the ion and neutral rapidly increase, so that the balance of attractive and repulsive contributions determines r_e . No simple picture is adequate to model the situation in the region around r_e . However, it can be seen that (thanks to a cancellation of errors) the extrapolated simple electrostatic curves give a surprisingly good first approximation to the actual binding energy of the system at r_e .

In a manner similar to Figure 1, Figure 2 shows the calculated MgCl⁺/benzene binding curve, along with electrostatic energy plots for point charges of charge +1.3 and +1.4. It is assumed that the ion approaches benzene along the symmetry axis with its Mg end pointing directly at the ring. The similarity of this figure to the comparisons shown in Figure 1 is notable, both in the fidelity of the electrostatic curves in modeling the approaching partners, and also in the way the actual curve deviates from the electrostatic model as the equilibrium binding distance is approached. Taking Figure 1 as our guide to how the “pure electrostatic” model should compare with the actual binding curve, we can conclude from Figure 2 that MgCl⁺ behaves in interacting with benzene very much as we would expect to observe for a hypothetical fractionally charged Mg ion with charge about +1.3 or +1.4. This thus gives a quantitative realization of the picture of MX⁺/benzene binding as a case intermediate between the extremes of M⁺ and M²⁺ binding. This

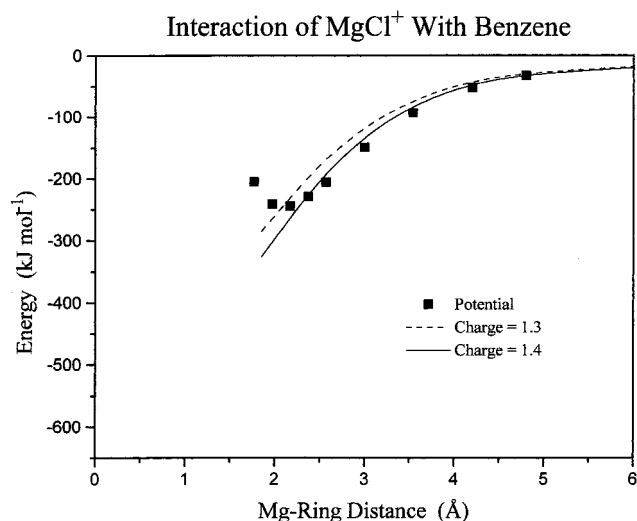


Figure 2. Interaction energies similar to Figure 1, for MgCl^+ with benzene. The electrostatic model calculations in this case are done by assigning a fictitious fractional charge to the point charge, which is placed at the position the Mg nucleus occupies in the actual complex.

intermediate character of MgCl^+ is equally reflected in the Mg–ring equilibrium distances shown in Table 2.

Conclusions

It is found that MCl^+ binds roughly half again as strongly to the aromatic face as the corresponding M^+ ion. This is true for all three metals, although the absolute magnitude of the binding energy decreases sharply in going from Mg to Ca to Sr as a consequence of decreasing electrostatic interaction. Bromide has a smaller effect on the binding ability of the metal center than chloride, in keeping with its lower electron-withdrawing ability. A second ligand attaches to most of these complexes, with a binding energy generally slightly less than that of the first ligand in the Ca and Sr systems, and much less in the Mg systems. The reduction in second-ligand binding energy is more pronounced for mesitylene, supporting the likelihood that it reflects steric crowding around the metal center in addition to electronic effects.

The present results encourage the point of view that MX^+ is a metal ion center with the charge of a monovalent alkaline earth but the electronic character of a divalent cation. The increase in formal oxidation of the metal center by the addition of the halide atom results in a large enhancement of the binding energy to the aromatic ligands studied here. Both the experimentally measured bond strength enhancement and the calculated shrinking of the metal–ring distance reflect the effect of the halogen in pulling the unpaired valence *s* electron away from the metal to allow more effective electrostatic interaction of the metal with the π face.

The gas-phase binding of MX^+ ions to the aromatic face is intermediate between the binding abilities of M^+ and M^{2+} . In the particular case of MgCl^+ , quantitative analysis via quantum chemical calculations indicates that this ion binds in a manner equivalent to a hypothetical magnesium center with fractional charge of +1.3 to +1.4.

Acknowledgment. The support of the donors of the Petroleum Research Fund, administered by the American Chemical Society, is gratefully acknowledged.

References and Notes

(1) Schröder, D.; Schwarz, H.; Clemmer, D. E.; Chen, Y.; Armentrout,

- P. B.; Baranov, V.; Böhme, D. K. *Int. J. Mass Spectrom. Ion Processes* **1997**, *161*, 175.
 (2) Brönstrup, M.; Schröder, D.; Schwarz, H. *Chem. Eur. J.* **1999**, *5*, 1176.
 (3) Kretzschmar, I.; Fiedler, A.; Harvey, J. N.; Schröder, D.; Schwarz, H. *J. Phys. Chem. A* **1997**, *101*, 6252.
 (4) Kretzschmar, I.; Schröder, D.; Schwarz, H.; Rue, C.; Armentrout, P. B. *J. Phys. Chem. A* **1998**, *102*, 10061.
 (5) Mandich, M. L.; Steigerwald, M. L.; Reents, W. D. *J. Am. Chem. Soc.* **1986**, *108*, 6197.
 (6) Mazurek, U.; Schröder, D.; Schwarz, H. *Collect. Czech. Chem. Commun.* **1998**, *63*, 1498.
 (7) Armentrout, P. B. *Acc. Chem. Res.* **1995**, *28*, 430.
 (8) Milburn, R. K.; Baranov, V.; Hopkinson, A. C.; Bohme, D. K. *J. Phys. Chem. A* **1999**, *103*, 6373.
 (9) Meyer, F.; Khan, F. A.; Armentrout, P. B. *J. Am. Chem. Soc.* **1995**, *117*, 9740.
 (10) Cerda, B. A.; Wesdemiotis, C. Presented at the 46th ASMS Conference on Mass Spectrometry and Allied Topics, Orlando, May 31–June 4, 1998.
 (11) Cooks, R. G.; Patrick, J. S.; Kotiaho, T.; McLuckey, S. A. *Mass Spectrom. Rev.* **1994**, *13*, 287.
 (12) Afzaal, S.; Freiser, B. S. *Chem. Phys. Lett.* **1994**, *218*, 254.
 (13) Sallans, L.; Laude, D. R.; Freiser, B. S. *J. Am. Chem. Soc.* **1989**, *111*, 1, 865.
 (14) Willey, K. F.; Cheng, P. Y.; Bishop, M. B.; Duncan, M. A. *J. Am. Chem. Soc.* **1991**, *113*, 4721.
 (15) Lin, C.-Y.; Dunbar, R. C. *J. Phys. Chem.* **1995**, *99*, 1754.
 (16) Faulk, J. D.; Dunbar, R. C. *J. Am. Chem. Soc.* **1992**, *114*, 8596.
 (17) Dunbar, R. C. New Approaches to Ion Thermochemistry via Dissociation and Association. In *Advances in Gas-Phase Ion Chemistry*; Babcock, L. M.; Adams, N. G., Eds.; JAI Press: Greenwich, CT, 1996; Vol. 2, p 87.
 (18) Dunbar, R. C.; McMahon, T. B. *Science* **1997**, *279*, 194.
 (19) Jockusch, R. A.; Schnier, P. D.; Price, W. D.; Strittmatter, E. F.; Demirev, P. A.; Williams, E. R. *Anal. Chem.* **1997**.
 (20) Schnier, P. D.; Price, W. D.; Jockusch, R. A.; Williams, E. R. *J. Am. Chem. Soc.* **1996**, *118*, 7178.
 (21) Thölmann, D.; Tonner, D. S.; McMahon, T. B. *J. Phys. Chem.* **1994**, *98*, 2002.
 (22) Tonner, D. S.; Thölmann, D.; McMahon, T. B. *Chem. Phys. Lett.* **1995**, *233*, 324.
 (23) Lin, C.-Y.; Dunbar, R. C.; Haynes, C. L.; Armentrout, P. B.; Tonner, D. S.; McMahon, T. B. *J. Phys. Chem.* **1996**, *100*, 19659.
 (24) Lin, C.-Y.; Dunbar, R. C. *J. Phys. Chem.* **1996**, *100*, 655.
 (25) Uppal, J. S.; Staley, R. H. *J. Am. Chem. Soc.* **1982**, *104*, 1235.
 (26) Dunbar, R. C. Review: Ion–Molecule Radiative Association. In *Current Topics in Ion Chemistry and Physics*; Ng, C. Y., Baer, T., Powis, I., Eds.; Wiley: New York, 1994; Vol. II.
 (27) Ryzhov, V.; Dunbar, R. C. *J. Am. Soc. Mass Spectrom.* **1999**, *10*, 862.
 (28) Ryzhov, V.; Dunbar, R. C. *J. Am. Chem. Soc.* **1999**, *121*, 2259.
 (29) Ryzhov, V.; Yang, C.-N.; Klippenstein, S. J.; Dunbar, R. C. *Int. J. Mass Spectrom.* **1998**, *185/186/187*, 913.
 (30) Lin, C.-Y.; Dunbar, R. C. *Organometallics* **1997**, *16*, 2691.
 (31) Ho, Y.-P.; Dunbar, R. C. *Int. J. Mass Spectrom.* **1999**.
 (32) Ho, Y.-P.; Yang, Y.-C.; Klippenstein, S. J.; Dunbar, R. C. *J. Phys. Chem.* **1997**, *101*, 3338.
 (33) Dunbar, R. C.; Klippenstein, S. J.; Hrušák, J.; Stöckigt, D.; Schwarz, H. *J. Am. Chem. Soc.* **1996**, *118*, 5277.
 (34) Klippenstein, S. J.; Yang, Y.-C.; Ryzhov, V.; Dunbar, R. C. *J. Chem. Phys.* **1996**, *104*, 4502.
 (35) Dunbar, R. C. *Int. J. Mass Spectrom. Ion Processes* **1997**, *160*, 1.
 (36) Herbst, E.; Dunbar, R. C. *Mon. Not. R. Astr. Soc.* **1991**, *253*, 341.
 (37) Dunbar, R. C. *Int. J. Mass Spectrom. Ion Processes* **1990**, *100*, 423.
 (38) Ryzhov, V.; Yang, Y.-C.; Klippenstein, S. J.; Dunbar, R. C. *J. Phys. Chem. A* **1998**, *102*, 8865.
 (39) Klippenstein, S. J.; Wagner, A. F.; Dunbar, R. C.; Wardlaw, D. M.; Robertson, S. H.; Diau, E. W. VariFlex computer code, available via anonymous FTP from london.tcg.anl.gov.
 (40) Frisch, M. J.; Trucks, G. W.; Schlegel, H. B.; Gill, P. M. W.; Johnson, B. G.; Robb, M. A.; Cheeseman, J. R.; Keith, T.; Petersson, G. A.; Montgomery, J. A.; Raghavachari, K.; Al-Laham, M. A.; Zakrzewski, V. G.; Ortiz, J. V.; Foresman, J. B.; Cioslowski, J.; Stefanov, B. B.; Nanayakkara, A.; Challacombe, M.; Peng, C. Y.; Ayala, P. Y.; Chen, W.; Wong, M. W.; Andres, J. L.; Replogle, E. S.; Gomperts, R.; Martin, R. L.; Fox, D. J.; Binkley, J. S.; Defrees, D. J.; Baker, J.; Stewart, J. P.; Head-Gordon, M.; Gonzalez, C.; Pople, J. A. *GAUSSIAN 94*; Gaussian, Inc.: Pittsburgh, PA, 1995.
 (41) Bauschlicher, C. W., Jr.; Partridge, H. *Chem. Phys. Lett.* **1991**, *181*, 129.